Interpreting the H/D Isotope Fractionation of Liquid Water during Evaporation without Condensation

ARTICLE *in* THE JOURNAL OF PHYSICAL CHEMISTRY C · APRIL 2007

Impact Factor: 4.77 · DOI: 10.1021/jp065095r

Interpreting the H/D Isotope Fractionation of Liquid Water during Evaporation without Condensation

Christopher D. Cappa,[†,‡,§] Jared D. Smith,[†,‡] Walter S. Drisdell,[†,‡] Richard J. Saykally,[†,‡] and Ronald C. Cohen*[,†,‡,||]

Department of Chemistry, University of California, Berkeley, California 94720-1460, Lawrence Berkeley National Laboratory, Berkeley, California 94720, and Department of Earth and Planetary Science, University of California, Berkeley, California 94720

Received: August 7, 2006; In Final Form: March 15, 2007

A theoretical model of liquid water evaporation has been developed to interpret results from a recent experimental investigation of isotope fractionation during free evaporation [Cappa et al. *J. Phys. Chem. B* **2005**, *109 (51)*, 24391]. It is established that the free evaporation isotope fractionation factors (α_{evap}) are primarily influenced by the nature of the intermolecular interactions between water molecules, namely, the condensed phase hindered translational and librational frequencies at the surface. The dependence of α_{evap} on the isotopic composition of the liquid can be understood in terms of small variations in these frequencies with isotopic composition. This result suggests that the explicit nature of the solvation environment directly influences evaporation rates from liquids. The sensitivity of the calculated evaporation coefficient for liquid water to both temperature and isotope composition is also explored.

1. Introduction

In a recent publication, we presented measurements of isotopic fractionation accompanying the free (collisionless) evaporation of liquid water.[1] The observed dependence of the free evaporation isotope fractionation factors (α_{evap}) on the isotopic composition of the liquid provided evidence that the evaporation coefficient (γ_e) for liquid water is less than unity. The evaporation coefficient is a physicochemical parameter describing the deviation of an observed evaporation rate ($J_{e,obs}$) from the theoretical maximum evaporation rate ($J_{e,max}$) given by the Hertz−Knudsen equation:

$$J_{e,max} = \frac{p_{sat}}{\sqrt{2\pi mkT}} \tag{1}$$

and

$$\gamma_e = \frac{J_e,obs}{J_{e,max}} \tag{2}$$

where p_{sat} is the saturation vapor pressure, m is the molecular mass, k is Boltzmann's constant, and T is temperature. The observation of an evaporation coefficient less than unity indicates the existence of an energetic or entropic barrier to evaporation, since $J_{e,obs}$ is traditionally interpreted in terms of an Arrhenius rate expression for the evaporation rate. In addition to the isotopic measurements, in a subsequent paper, we reported on measurements of the temperature changes associated with freely evaporating water droplets, the results of which suggested that the evaporation coefficient for pure liquid water is ~0.6 and has at most a relatively small dependence on temperature.[2] In contrast, various other modern measurements have suggested that the mass accommodation coefficient of water vapor onto liquid water (defined in an apparently equivalent way as the evaporation coefficient, cf. eq 2) has a negative temperature dependence, ranging from 0.32 to 0.17 over 258−280 K,[3] is 0.06[4] or is unity.[5] Clearly, clarification regarding the actual value and temperature dependence of the evaporation/mass accommodation coefficient is needed.

For isotopic water mixtures, the evaporation fractionation factor, α_{evap}, can be formulated in terms of the ratio between the individual evaporation rates of the different isotopic species such that[1]

$$\alpha_{evap} = \frac{R_{evap}}{R_{liq}} = \frac{A_L(T)}{A_H(T)} e^{-\Delta E_a / RT} \tag{3}$$

where R_x is the isotopic ratio in the evaporate or the liquid, A_X is the Arrhenius pre-factor, and ΔE_a is the difference in the activation energy for evaporation between the respective isotopomers. Assuming A to be independent of temperature, a fit to measurements of α_{evap} for a $\chi_D = 0.5$ isotopic water solution over the range 268 K < T < 295 K resulted in the parameters $\Delta E_a = -1.8 \pm 0.3$, -3.6 ± 0.4, and -1.8 ± 0.2 kJ/mol, and $A_L/A_H = 0.6 \pm 0.1$, 0.4 ± 0.1, and 0.6 ± 0.1 for H_2O/HDO, H_2O/D_2O, and HDO/D_2O fractionation, respectively.

To provide a more complete interpretation of the physical basis for the experimental observations of the composition and temperature dependence of α_{evap}, a transition state theory (TST) model is developed that helps elucidate the important microscopic interactions in liquid water that control the evaporation process. This model provides for a rationalization of the observed dependence of α_{evap} on the isotopic composition of the liquid. Specifically, variation of the intermolecular interactions among neighboring water molecules at the liquid surface with changing isotopic composition is identified as the primary

* Corresponding author.
† Department of Chemistry.
‡ Lawrence Berkeley National Laboratory.
§ Present address: NOAA Earth System Research Laboratory, Chemical Science Division, Boulder, Colorado 80305.
|| Department of Earth and Planetary Science.

10.1021/jp065095r CCC: $37.00
Published on Web 04/24/2007

TABLE 1: Vibrational Spectroscopic Properties and Rotational Temperatures[8,9] for Gas-Phase H_2O, HDO, and D_2O and the Calculated Transition State Partition Functions and Partition Function Ratios at 295 K[a]

	H_2O	HDO	D_2O
mass (kg)	2.99×10^{-26}	3.16×10^{-26}	3.33×10^{-26}
σ	2	1	2
υ_1 (cm^{-1})	3657.05	2723.66	2671.46
υ_2 (cm^{-1})	1594.59	1402.2	1178.33
υ_3 (cm^{-1})	3755.97	3707.47	2788.05
θ_A (K)	40.1	33.6	22.1
θ_B (K)	20.9	13.1	10.5
θ_C (K)	13.4	9.2	7.0
q_υ^*	1.0004	1.0011	1.0032
q_r^*	42.4	140.8	111.7
q_t^*	3.75	3.96	4.17

ratios	H_2O/HDO	H_2O/D_2O	HDO/D_2O
$q^*_{\upsilon,L}/q^*_{\upsilon,H}$	0.999	0.997	0.998
$q^*_{r,L}/q^*_{r,H}$	0.301	0.380	1.260
$q^*_{t,L}/q^*_{t,H}$	0.95	0.90	0.95
Q^*_L/Q^*_H	0.285	0.341	1.194

[a] Individual vibrational, rotational, and translational contributions to the total transition state partition function are considered. q_t^* was calculated assuming *area* $= 2.15 \times 10^{-21}$ m^2.

control on α_{evap}. Also, the model results indicate that the pre-factor ratio may not actually be temperature independent and therefore that it is necessary to revisit the previous interpretation of the observed $\alpha_{evap}(T)$. Finally, the model is used to explicitly calculate γ_e for liquid water and to explore the dependence on temperature and isotopic composition.

2. Transition State Model of Evaporation

Transition state theory is used to develop a microphysical interpretation of the pre-factor ratio and ΔE_a, following the approach of Smith et al.[6] The TST rate of desorption is given by

$$J_{e,x} = [X]_{surf} \frac{kT}{h} \frac{Q^*}{Q_s} e^{-E_a/kT} \tag{4}$$

where Q^* and Q_s are the partition functions (PF) for the transition state and the liquid surface species, respectively. E_a is the activation energy for evaporation of species X. For isotopic species, the above equation can be used to give the isotope ratio:

$$\alpha_{evap} = \frac{J_{e,L}}{J_{e,H}} \frac{[H]_{surf}}{[L]_{surf}} = \frac{A_L}{A_H} e^{-\Delta E_a/kT} = \frac{Q^*_L}{Q^*_H} \frac{Q^H_s}{Q^L_s} e^{-\Delta E_a/kT} \tag{5}$$

We assume here, as we have done previously,[1] that the surface isotopic composition is equal to that of the bulk liquid. This assumption, as it relates to interpretation of our prior measurements, is discussed further in Appendix A.

2.1. Pre-factor: Partition Function Ratios for the Transition State and Surface Species. For α_{evap}, the total pre-factor ratio depends on the ratio of the transition state PFs and on the ratio of the surface species PFs (eq 5). Although the surface species is reasonably easy to define, it is important that an unambiguous choice of the activated complex is made. The activated complex should be chosen so as to minimize the flux back across the transition state. If the potential energy between the evaporating molecule and the surface increases monotonically with distance to infinity, then this requirement necessitates that the activated complex exist at infinite separation from the surface, that is, corresponding to a free gas-phase molecule.[7] However, if there is an energy barrier to evaporation, then this is only an approximate representation of the actual activated complex. In the absence of specific knowledge of the nature of the transition state during evaporation of water, we will use the approximation that the activated complex is equivalent to a free molecule with one translational degree of freedom removed. Q^* can be expressed in terms of the vibrational, rotational, and translational contributions as $Q^* = q_v^* q_r^* q_t^*$. The partition function for the intramolecular vibrations (assuming the vibrations can be treated as harmonic oscillators) is

$$q_v^* = \prod_{i=1}^{n} \left(1 - e^{-(h\upsilon_i/kT)}\right)^{-1} \tag{6}$$

where υ_i is the vibrational frequency of the ith mode, and for water $n = 3$. The characteristic intramolecular fundamental frequencies of gas-phase H_2O, HDO, and D_2O are well-known (Table 1).[8,9]

The partition function for the free rotations is[10]

$$q_r^* = \frac{\sqrt{\pi}}{\sigma} \sqrt{\frac{T^3}{\theta_A \theta_B \theta_C}} \tag{7}$$

Here, σ is the symmetry factor. θ_x is the rotational temperature about each of the principal axes given by

$$\theta_x = \frac{h^2}{8\pi^2 I_x k} \tag{8}$$

where I_x is the moment of inertia about the x axis. The rotational temperatures for the three isotopomers are well-known (Table 1).[8,9] The symmetry factor is 2 for H_2O (D_2O) owing to the indistinguishability of the hydrogen atoms (deuterium atoms), but for HDO $\sigma = 1$.

The PF for the two-dimensional (2D) free translation is[10]

$$q_t^* = \frac{2\pi mkT}{h^2} area \tag{9}$$

where m is the molecular mass and *area* is the area of the 2D transition state. The term *area* is not well constrained; however, when considering only the isotope ratios, *area* will cancel, and it is thus unnecessary to define it further at this point. The above expression for q_t^* is for only two degrees of freedom, as the third is the desorption coordinate. Combining eqs 6, 7, and 9 gives the total PF ratio for isotopomers at the transition state:

$$\frac{Q^*_L}{Q^*_H} = \frac{m_L}{m_H} \frac{\sigma_H}{\sigma_L} \left(\frac{\theta^H_A \theta^H_B \theta^H_C}{\theta^L_A \theta^L_B \theta^L_C}\right)^{1/2} \prod_{i=1}^{3} \left(\frac{1 - e^{-h\upsilon_i^H/kT}}{1 - e^{-h\upsilon_i^L/kT}}\right) \tag{10}$$

The individual contributions from the q_t^*, q_r^*, and q_v^* terms, as well as the total ratios, are given in Table 1.

It is more difficult to calculate the PF for the surface species, Q_s, because the rotational and translational motions can no longer be considered free. Instead, the surface species exhibits frustrated rotational (librational) and hindered translational motions due to the strong interactions between neighboring molecules. We treat these intermolecular motions in the same way as the intramolecular vibrations and calculate the PFs as

in eq 6, within the harmonic approximation. This results in a total surface species isotopomer partition function ratio,

$$\frac{Q_s^L}{Q_s^H} = \frac{\sigma_H}{\sigma_L}\frac{q_{s,v}^L q_{s,r}^L q_{s,t}^L}{q_{s,v}^H q_{s,r}^H q_{s,t}^H} = \frac{\sigma_H}{\sigma_L}\prod_{i=1}^{9}\left(\frac{1-e^{-(h\nu_i^H/kT)}}{1-e^{-(h\nu_i^L/kT)}}\right) \quad (11)$$

where the product is now over the three intramolecular modes and the six intermolecular modes. The differing symmetry numbers of the water isotopomers are explicitly considered in the total condensed phase PF because the ratio of symmetry numbers cannot itself lead to isotopic enrichment,[11] and must therefore cancel with the symmetry number ratio in the transition state PF ratio. In calculations of α_{evap}, we might expect that corrections due to anharmonicity of the molecular motions might cancel when calculating the ratios and that the harmonic approximation is therefore a reasonable estimate.[12] For example, use of the harmonic approximation to calculate the $H_2O + D_2O = 2HDO$ gas-phase equilibrium constant yields nearly identical results as if anharmonicity corrections are taken into account.[13] However, when PF ratios are not used (i.e., when the absolute values of the PFs are important), it may be necessary to account for anharmonicity to obtain quantitatively correct results, in particular, for the librational and hindered translational motions in the liquid. As a first approximation, we will use the bulk liquid frequencies for the surface species. This approximation will be addressed further below.

The liquid phase intramolecular vibrational frequencies for H_2O and D_2O are difficult to accurately specify owing to the complexity of both the Raman and infrared spectra. To quantitatively fit the H_2O and D_2O Raman spectra, it is necessary to treat them as if they represented at least a four component system (i.e., a minimum of four Gaussians must be used representing *n* different hydrogen-bonding configurations).[14] In contrast, the vibrational Raman spectrum of liquid HDO (as either HDO in D_2O or in H_2O) can be well fit by only two Gaussian components. However, it is important to note that the center of these Gaussian-like components should not be interpreted strictly as the υ_1 and υ_3 frequencies of water molecules in solution but rather arise because of the spectral overlap from a continuous distribution of different hydrogen-bonded structures and the asymmetry of the intermolecular bonding potential.[14]

As an approximation, the υ_1 and υ_3 vibrational frequencies (υ_ν) for HDO are taken as the band centers of the main Gaussian components at 295 K of the −OH spectrum (in D_2O) at 3436 cm^{-1} and the −OD spectrum (in H_2O) at 2525 cm^{-1}.[15] (These liquid-phase frequencies are both 92.7% of the well-known gas-phase HDO fundamentals, indicating equivalent shifts upon condensation.) To maintain consistency between the choice of υ_ν for HDO (where the higher energy Gaussian component has been ignored for both the −OD and −OH stretches) and those for H_2O and D_2O, we use for both υ_1 and υ_3 of H_2O and D_2O the band center of the Gaussian component that corresponds to the intensity maximum in a four Gaussian fit, which are 3450 cm^{-1} and 2507 cm^{-1} at 295 K, respectively.[15] In other words, both H_2O and D_2O are treated in terms of an average condensed phase species that corresponds approximately to the maximum in the hydrogen-bond length probability distribution.[14] The υ_2 bending frequencies for all three species are more easily identified from both the Raman and the infrared spectrum and are given in Table 2.[16] We note that sum frequency generation vibrational spectra of the liquid water surface suggest that a significant fraction of molecules at the surface exist with one OH bond oriented toward the vapor.[17] These "free" OH bonds give rise to a sharp feature at higher energies (e.g., ~3700 cm^{-1} for H_2O). We have found that if the free OH or OD stretching frequency is used in place of one of the above condensed phase vibrational frequencies, then the details of our calculation are changed somewhat, but the general conclusions of this study remain valid.

TABLE 2: Inter- and Intramolecular Frequencies Used to Calculate the Surface Species Partition Functions and Isotope Ratios (light/heavy) at 295 K[a]

	H_2O (cm^{-1})	**HDO** (cm^{-1})	**D_2O** (cm^{-1})
υ_1	3450	3436	2507
υ_2	1645	1450	1235
υ_3	3450	2525	2507
$\upsilon_{r,1}$	470	410	350
$\upsilon_{r,2}$	570	498	425
$\upsilon_{r,3}$	760	665	570
$\upsilon_{t,1}$	175	*170*	*169*
$\upsilon_{t,2}$	60	*55*	*54*
$\upsilon_{t,3}$	290	*285*	*284*
ratios	**H2O/HDO**	**H2O/D2O**	**HDO/D2O**
$q_{s,\upsilon}^L/q_{s,\upsilon}^H$	0.999	0.998	0.998
$q_{s,lib}^L/q_{s,lib}^H$	0.921	0.816	0.886
$q_{s,ht}^L/q_{s,ht}^H$ [b]	0.899	0.890	0.989
Q_s^L/Q_s^H [b]	0.414	0.725	1.751
Q_s^L/Q_s^H [c]	0.460	0.814	1.769

[a] Italicized values of υ_{ht} (for HDO and D_2O) were tuned to obtain absolute agreement with the experimentally observed pre-factor ratios at $\chi_D = 0.5$ (see text for details). [b] Uses $\upsilon_{t,s}$ values given above. [c] Assumes $\upsilon_{t,s}(H_2O) = \upsilon_{t,s}(HDO) = \upsilon_{t,s}(D_2O)$.

The librational frequencies of H_2O and D_2O ($\upsilon_{lib} \sim 300-1000$ cm^{-1}) used are given in Table 2.[18] As with the vibrational frequencies, given the broad nature of the experimental spectra in this region, the values used are only approximates. Determination of the pure HDO υ_{lib} is not currently possible, and we therefore use for HDO the average of the H_2O and D_2O υ_{lib}. These estimates of υ_{lib} for H_2O and D_2O were determined from pure liquid H_2O and D_2O; their dependence on isotopic composition, in particular at the surface, is not explicitly known.

The actual frequencies of the three low-frequency hindered translations (υ_{ht}) are poorly constrained for the isotopic species. Measurements of the Raman spectrum of liquid H_2O indicate that two broad features exist, centered at ~60 cm^{-1} and 175 cm^{-1}.[18,19] The third hindered translation has not been unambiguously identified but is thought to lie at ~290 cm^{-1}.[18] For the isotopic variants, the υ_{ht} are thought to lie close in energy to those of H_2O,[18] although they may be slightly (~5−10 cm^{-1}) lower. As with the librations, it is unknown how the υ_{ht} specifically depend on isotopic composition. As a first approximation, we use the same υ_{ht} for all three isotopic species. The condensed phase frequencies and q_x values are reported in Table 2.

Using the frequencies and rotational constants given in Table 1 and Table 2, we calculated the individual Q's and A_L/A_H (Table 3). The calculated A_L/A_H exhibits a non-negligible dependence on temperature. Our previous analysis[1] based on the assumption that A was approximately constant over the temperature range $268\ K < T < 295\ K$ thus leads to an unrealistic physical picture of evaporation.

One further consideration is the appropriateness of using bulk liquid frequencies to approximate the surface species frequencies. Smith et al. have suggested scaling the bulk librational and hindered translational frequencies by $\sqrt{3/4}$ to account for looser binding at the surface which will accompany the

TABLE 3: Calculated Total ($Q_L^* Q_s^H / Q_H^* Q_s^L$) and Vibrational, Rotational, and Translational ($q_L^* q_s^H / q_H^* q_s^L$) Partition Function Ratios at 295 K Using the Parameters from Table 2

ratios	H_2O/HDO	H_2O/D_2O	HDO/D_2O
vib	1.00	1.00	1.00
rot	0.33	0.47	1.42
trans[a]	1.05	1.01	0.96
trans[a]	0.95	0.90	0.95
total[a]	0.69	0.47	0.68
total[b]	0.62	0.42	0.67

[a] Uses $\upsilon_{t,s}$ values reported in Table 2. [b] Assumes $\upsilon_{t,s}(H_2O) = \upsilon_{t,s}(HDO) = \upsilon_{t,s}(D_2O)$.

decreasing number of hydrogen bonds formed per molecule.[6] Since the proper choice is ambiguous, we use both the bulk liquid and the scaled "surface" frequencies in these calculations.

2.2. Activation Energy, E_a. E_a for evaporation can be approximated as the difference between the zero point (ZP) corrected total energy of the loosely bound surface species and the ZP corrected energy of the activated complex, that is, $E_a = E_c + ZPE^* - ZPE_s$ (see Figure 1).[6] Within the Born−Oppenheimer approximation, the ZPE uncorrected desorption energy (E_c) is identical for the different isotopomers. When dealing with isotopic fractionation it is necessary to have knowledge only of the difference in E_a between the isotopomers, and not of the absolute values of E_a or E_c alone. Hence,

$$\Delta E_a = (E_c + ZPE^*_L - ZPE_s{}^L) - (E_c + ZPE^*_H - ZPE_s{}^H) = (ZPE_s{}^H - ZPE_s{}^L) + (ZPE^*_L - ZPE^*_H) = -\Delta ZPE_s + \Delta ZPE^* \quad (12)$$

The total ZPE contributions from each oscillator were estimated as

$$ZPE = \frac{1}{2}\sum_{i=1}^{n} h\upsilon_i \quad (13)$$

where the sum is over the three intramolecular vibrations for the activated complex and over the three intra- and six intermolecular vibrations for the surface species.[6] Although the major contribution to the total ZPE_s is from the intramolecular vibrations, the ΔE_a depends on the differences in vibrational, librational, and hindered translational motions between isotopomers. The calculated ZPE exhibits equal sensitivity to composition-dependent shifts in any of the frequencies. For example, changing any one of the frequencies of a single isotopomer by 10 cm^{-1} corresponds to a change in the calculated ΔE_a of 0.18 kJ/mol

2.3. Calculation of α_{evap}. α_{evap} values for H_2O/HDO, H_2O/D_2O, and HDO/D_2O were determined from eq 3 using the calculated A_L/A_H and ΔE_a. Using the molecular parameters directly from Table 1 and Table 2 (either scaled or un-scaled), we find that the calculated α_{evap} are within the range of previously measured values.[1] In the following sections, the calculated isotope composition dependence and the calculated temperature dependence of the α_{evap} are explored.

2.3.1. Isotope Composition Dependence. The measured α_{evap} were found to exhibit a very strong dependence on isotopic composition.[1] Given the relatively high sensitivity of the calculated A_L/A_H and ΔE_a to changes in the specified condensed phase frequencies, exact agreement between the measured and the calculated α_{evap} at every χ_D can be obtained by allowing for isotope composition-dependent shifts in the condensed phase

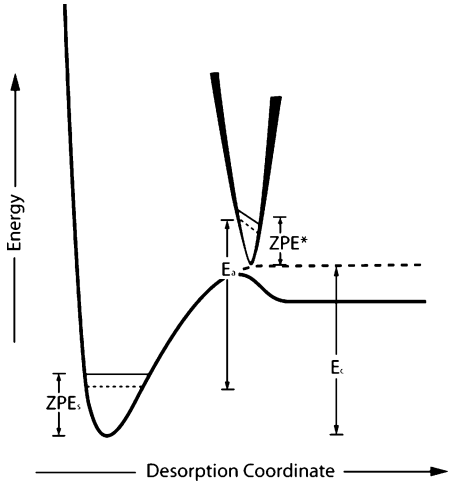

Figure 1. Energy diagram for the evaporation of a water molecule from the liquid surface. The ZPE of the light isotopomers is indicated as a solid line, and the ZPE of the heavy isotopomers is indicated by the dashed line. The activation energy depends on the ZPE difference between the activated complex (ZPE^*) and the surface species (ZPE_s) and on the classical desorption energy (E_c). Although there may be an intrinsic kinetic barrier to evaporation (indicated by the solid curve), because the transition state was specified as the gas phase, in the model presented herein, there is formally no barrier to evaporation (as indicated by the dashed curve).

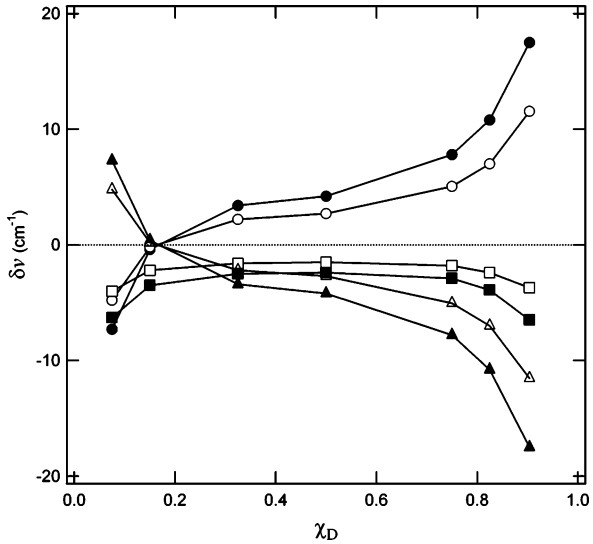

Figure 2. The frequency shifts ($\delta\upsilon$) necessary to bring the calculated α_{evap} into agreement with previous measurements [ref 1] for (●) H_2O, (■) HDO, and (▲) D_2O, under the assumption that $\delta\upsilon(H_2O) = -\delta\upsilon(D_2O)$. The scaled frequencies were used. Solid symbols correspond to when the $\delta\upsilon$ are for the hindered translational frequencies only, and open symbols correspond to when the $\delta\upsilon$ are for all of the condensed phase frequencies.

frequencies. Because A_L/A_H is most sensitive to changes in the υ_{ht}, we first considered the frequency shifts ($\delta\upsilon_{ht}$) necessary to bring the calculated α_{evap} into agreement with experiment (Figure 2). All of the $\delta\upsilon_x$ are referenced to the υ_x given in Table 2. As a first case, it was assumed that $\delta\upsilon_{ht}(H_2O) = -\delta\upsilon_{ht}(D_2O)$, and the $\delta\upsilon_{ht}$(HDO) were subsequently determined. Alternatively, simultaneous shifts in υ_{ht}, υ_v, and υ_{lib} were considered. When simultaneous, equivalent shifts in all three are allowed (i.e., $\delta\upsilon_{ht} = \delta\upsilon_{lib} = \delta\upsilon_{vib}$), the associated shift in any given υ_x becomes smaller.

These results indicate that the observed variation in α_{evap} with χ_D may be driven by relatively small shifts of the frequencies

associated with the surface species with changing isotopic composition. Specifically, the differences in the frequencies ($\upsilon_x^L - \upsilon_x^H$) between the isotopic species must vary with χ_D.

Although it is not possible to critically assess whether frequency shifts in υ_{ht}, υ_{lib}, or υ_v are most important, we believe that variations in υ_{ht} and υ_{lib} with isotopic composition are most probable. If correct, this implies that the librational and hindered translational motions of surface-bound molecules play a crucial role in determining molecular evaporation rates of liquids. For water, these motions are primarily controlled by the nature of hydrogen-bonding interactions between neighboring water molecules. Hydrogen bonding between different isotopic species will depend explicitly on the composition of the solution, as the nature of both the donor and acceptor hydrogen bonds depend upon this.

It is of interest that the $\delta\upsilon$ for H_2O and D_2O required to match the experimental observations vary strongly with χ_D, whereas $\delta\upsilon$ for HDO is nearly constant over the entire composition range, although $\delta\upsilon$(HDO) does decrease slightly at both high and low χ_D compared with the value at $\chi_D = 0.5$. The specific behavior of HDO can be contrasted with that of H_2O (D_2O) where $\delta\upsilon$ increases (decreases) monotonically with increasing χ_D. It is possible that this difference between HDO and H_2O/D_2O results from differences in the variation in the abundance of these species in the liquid with χ_D. H_2O and D_2O abundances both decrease monotonically from their respective pure liquids, whereas the HDO abundance is maximum at $\chi_D = 0.5$ and decreases at both lower and higher χ_D. Despite these differences, $\delta\upsilon^L - \delta\upsilon^H$ increases with χ_D for all isotopic pairs.

Unlike our measurements of α_{evap}, it has been suggested that the variation in the equilibrium fractionation factor, α_{eqm}, for water with isotopic composition is quite small.[20] Yet, the sensitivity of our calculation of α_{eqm} to frequency differences in different isotopic mixtures is similar to that for α_{evap} because both are formulated similarly. (See Appendix B for a detailed description of the calculation of α_{eqm}). This then indicates that the behavior of the bulk condensed phase molecules with respect to changing isotopic composition is very different from that of the surface molecules, particularly for the hindered translational and librational motions. Although perhaps surprising, we believe such a conclusion to be reasonable given the very different local environments of the surface relative to the bulk liquid. For example, the water molecules at the liquid surface are known to be more strongly oriented than those in the bulk,[17] and as a result, their associated dynamics probably occur on significantly longer time scales.[21] Therefore, it is possible that isotopic substitution may influence the relative behavior of surface molecules quite differently than bulk molecules.

Recall that when considering fractionation it is not just important whether, for example, a H_2O molecule in H_2O behaves differently than one in D_2O (as is likely) but whether there is a change *relative* to the other isotopic species. Clearly, whether an evaporation event occurs or not will depend importantly on the specific orientation of water molecules at the surface. A molecule that makes two donor hydrogen bonds is probably less likely to evaporate than a molecule that makes only one hydrogen bond, given equivalent numbers of acceptor bonds. Therefore, any potential changes in the relative hydrogen bonding of surface bound molecules with isotopic composition will be important in determining the extent of fractionation during free evaporation.

2.3.2. Temperature Dependence. The temperature dependence of α_{evap} was also calculated, assuming, as a first approximation, that the frequencies do not vary with temperature. The calculated α_{evap} decrease with temperature, which is consistent with experiment. The slope and intercept from a plot of the calculated ln α_{evap} versus $1/RT$ can be quantitatively compared with experiment (Table 4). The experimental values were determined for a $\chi_D = 0.5$ solution, and therefore $\alpha_{evap}(T)$ was calculated with the $\delta\upsilon_{ht}$ chosen to give agreement with the measured α_{evap}(295 K). If the difference in the frequencies between isotopomers does vary with temperature, then this will affect the details but not the general aspects of the calculations.

TABLE 4: Calculated Activation Energy Differences for the Water Isotopomers (ΔE_a) and the (Negative) Slopes and Exponentials of the Intercepts of the Calculated ln α_{evap} vs $1000/RT$

	unscaled/unshifted frequencies		
	H_2O/HDO	**H_2O/D_2O**	**HDO/D_2O**
ΔE_a (kJ/mol)	−1.12	−2.28	−1.16
−slope (kJ/mol)	−0.80	−1.55	−0.76
exp(intercept)	0.71	0.56	0.80
	unscaled/shifted frequencies		
ΔE_a (kJ/mol)	−1.21	−2.38	−1.17
−slope (kJ/mol)	−0.83	−1.60	−0.77
exp(intercept)	0.83	0.70	0.84
	scaled/unshifted frequencies		
ΔE_a (kJ/mol)	−0.94	−1.92	−0.98
−slope (kJ/mol)	−0.59	−1.14	−0.55
exp(intercept)	0.73	0.60	0.82
	scaled/shifted frequencies		
ΔE_a (kJ/mol)	−1.06	−2.07	−1.01
−slope (kJ/mol)	−0.62	−1.19	−0.57
exp(intercept)	0.91	0.83	0.92
	experimental[a]		
−slope (kJ/mol)	−1.8 ± 0.6	−3.6 ± 0.8	−1.8 ± 0.4
exp(intercept)	0.6 ± 0.2	0.4 ± 0.2	0.6 ± 0.2

[a] For a $\chi_D = 0.5$ solution, ref 1, 2σ error.

The calculated intercepts, using either scaled or un-scaled frequencies, exhibit reasonable agreement with the measured values. The calculated slopes are generally smaller than the measured values, although the variation in the calculated values agrees with the observed dependence upon the isotope ratio considered (i.e., the slope for H_2O/HDO ∼ HDO/D_2O ∼ 0.5 × H_2O/D_2O).[1] Thus, we find overall modest agreement between these calculations and the observed T and χ_D dependence of α_{evap}.

Because the pre-factor ratio increases with increasing temperature, the variation of the calculated α_{evap} with temperature is weaker than that expected based solely on the calculated ΔE_a values (see Table 4). Note that even though the pre-factor ratio is temperature dependent, the plot of ln α_{evap} versus $1/RT$ is highly linear (Figure 3). This is because, over the considered temperature range (260−300 K), the pre-factor ratio varies approximately exponentially with temperature.

2.4. Absolute Desorption Rates and γ_e. In the above discussion, the focus has been on the determination of the relative rates of evaporation for the different water isotopomers, that is, of α_{evap}. We also calculate the absolute evaporation rates, although these calculations are much more sensitive to the details of the model than are the isotope ratios. However, to carry out this comparison, it is necessary to have knowledge of both the

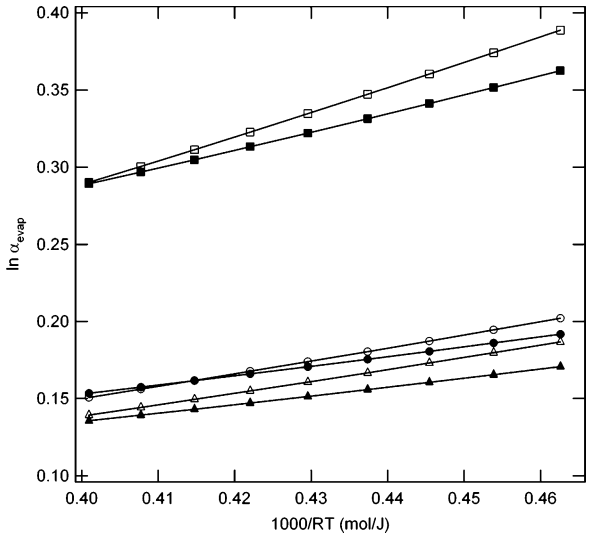

Figure 3. Calculated *T* dependence of α_{evap} for (●) H_2O/HDO, (■) H_2O/D_2O, and (▲) HDO/D_2O fractionation using bulk (open) and scaled (solid) frequencies. The hindered translational frequencies were shifted to give agreement with the measurements of α_{evap} for a $\chi_D = 0.5$ solution from ref 1.

classical desorption barrier, E_c (or the experimentally determined E_a), and the effective area of the transition state, *area*, which determines the magnitude of the activated complex translational PF. (Neither of these values need to be known explicitly when considering the isotope ratio measurements). Unfortunately, neither E_c nor *area* are known a priori.

Recent measurements from our laboratory demonstrated that, for pure H_2O, $\gamma_e \sim 0.6$ at 275 K.[2] Furthermore, γ_e was shown to exhibit, at most, a weak dependence on temperature. These experimental results can be used to constrain and explore the calculated behavior of γ_e by providing a reference point from which E_c and *area* can be determined. E_c and *area* were therefore chosen so as to give $\gamma_e(H_2O) = 0.6$ at 280 K; a surface concentration of $\theta = 1 \times 10^{15}$ molecules/cm^2 was used[6,22] along with the scaled frequencies, where $\delta\upsilon = 0$. Under these conditions $E_a = E_c - 9.3$ kJ/mol.

2.4.1. Temperature Dependence. The *T* dependence of γ_e for H_2O was explored as a function of the specified classical desorption energy, where E_c has been adjusted in 5 kJ/mol intervals (Figure 4). Using the scaled frequencies, when $E_c <$ 51 kJ/mol ($E_a <$ 41.7 kJ/mol), we found the calculated γ_e decreases with increasing temperature, whereas when $E_c >$ 51 kJ/mol, γ_e increases with increasing temperature. If the un-scaled frequencies are instead used, this changeover point is 52.2 kJ/mol ($E_a = 41.1$ kJ/mol). Note that for all E_c considered, the calculated evaporation rates increase with temperature, as is expected (Figure 4). Our prior experiments[2] indicated that γ_e varies only modestly with temperature, and the results were generally inconsistent with a value of γ_e that decreased with increasing temperature. Nearly exact agreement with the weak observed *T* dependence of γ_e is found when $E_c = 51$ kJ/mol (*area* $= 2.45 \times 10^{-21}$ m^2). Interestingly, when $E_c = 51$ kJ/mol, the *T* dependence of the calculated evaporation rate (considered as the slope of a plot of ln J_e vs $1/RT$) is 43.7 kJ/mol, very similar to the enthalpy of vaporization for liquid water. This calculated slope is smaller by ~10 kJ/mol than that previously measured by monitoring the absolute signal level decrease of the evaporate measured from a rapidly cooling, freely evaporating liquid jet.[1] However, it was pointed out at the time that the measurements of the absolute evaporation rates

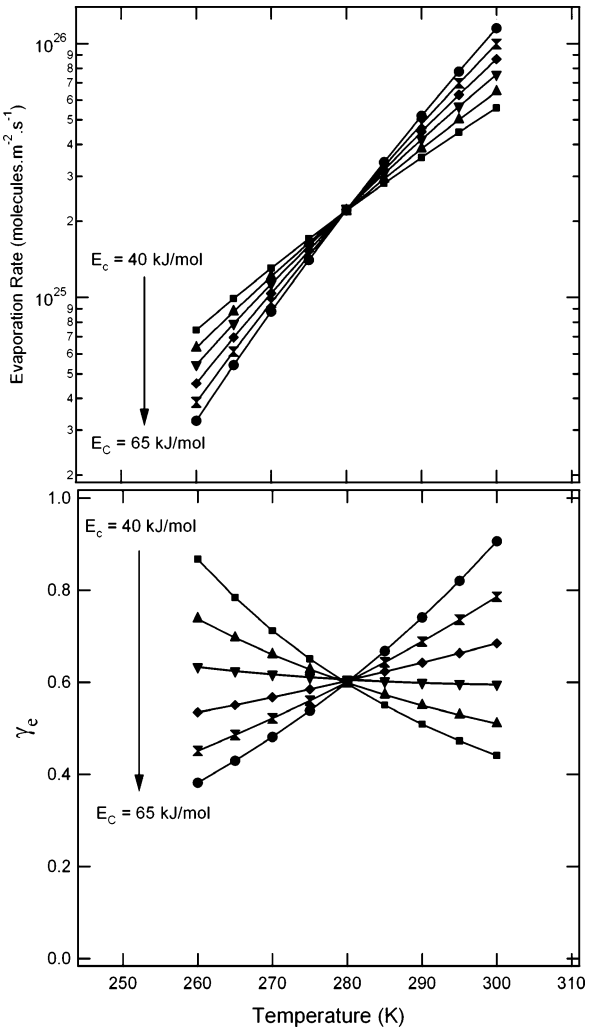

Figure 4. (a) *T* dependence from 260 to 300 K of the calculated H_2O evaporation rate as a function of the specified classical desorption barrier from 40 to 65 kJ/mol, in 5 kJ/mol increments (black lines). The theoretical maximum evaporation rate, from the Knudsen equation with $\gamma_e = 1$, is shown for comparison (gray line). Note the log scale on the *y* axis. (b) The calculated *T* dependence of γ_e for H_2O as a function of the specified classical desorption barrier from the rates shown in (a). In all cases, *area* was chosen such that $\gamma_e(280\text{ K}) = 0.6$ and scaled frequencies have been used. Note the change from a positive to negative dependence on temperature when $E_c \sim 51$ kJ/mol.

(as opposed to the isotopic ratio measurements) were subject to fairly large uncertainties beyond the precision of the measurement that were associated primarily with accurate control of the liquid jet position and which may have led us to significantly over-estimate the slope from the measurements.

In the above analysis it was assumed that the υ_x are temperature independent. However, they are likely to vary to some extent with temperature. The specific *T* dependence for any given υ_x is not explicitly known for temperatures below ~295 K, but extrapolation of the high-temperature results suggests that the librational and hindered translational frequencies tend to increase, to varying extents, with decreasing temperature, with the exception of the lowest energy hindered translation for which υ_{ht} apparently decreases with temperature.[23] From this, the potential influence of having *T*-dependent υ_x can be assessed in a general manner. If all of the υ_x increase with decreasing temperature, the calculated γ_e will increase with decreasing temperature, when $E_c = 51$ kJ/mol. However, it is possible to choose E_c such that the calculated γ_e is nearly

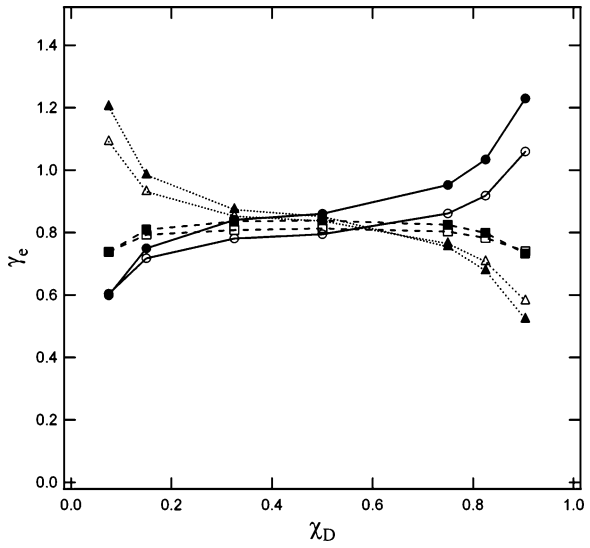

Figure 5. Calculated variation of γ_e with deuterium mole fraction for (●) H_2O, (■) HDO, and (▲) D_2O using the $\delta\upsilon_{ht}$ as specified in Figure 2. Solid symbols are for frequency shifts only in υ_{ht}, and open symbols are for shifts in both υ_{ht} and υ_{lib}. Scaled frequencies have been used.

temperature independent, even if the υ_x vary with temperature. For example, if the υ_x all increase with decreasing temperature, then the E_c required to have a γ_e that is temperature independent is greater than 51 kJ/mol, and vice versa.

It is also of interest to consider the model results when E_c and *area* are selected so as to be generally consistent with the determined negative temperature dependence of the mass accommodation coefficient of water on liquid water by Li et al.[3] Agreement with the temperature-dependent variation in the mass accommodation coefficient reported by Li et al. (0.32−0.17 over the range 258−280 K) can be obtained using E_c = 34 kJ/mol, corresponding to E_a = 24.7 kJ/mol (with *area* = 4.7×10^{-25} m^2). Using these parameters, the slope of a plot of ln J_e versus $1/RT$ is quite small, only 26.7 kJ/mol. It should be noted that the T dependence of the calculated γ_e does not have the same low-temperature limiting behavior as that reported for the mass accommodation coefficient[3] and that the E_c was selected to give agreement only over the measured temperature range. At this point, the reason for the discrepancy in the T dependence suggested by our evaporation measurements[2] and by the uptake studies of Li et al. is unknown. Without explicit knowledge of E_c and *area*, it is not possible to establish, through use of this model, the validity of the temperature dependencies as deduced from the two experiments. It is, however, important to carefully assess the temperature dependence of γ_e because, if γ_e were to become less than ∼0.1 for some temperatures, it may become important in determining the formation rates and lifetimes of atmospheric clouds.[24,25] However, the Smith et al. measurements[2] appear to rule out this possibility, and the Li et al. results[3] indicate that the mass accommodation coefficient is less than 0.1 only at T > 295 K, where cloud formation is unimportant.

2.4.2. Composition Dependence. Because α_{evap} varies with χ_D, it is necessary that the γ_e for each of the isotopic species also vary with χ_D. Starting with the assumption that γ_e = 0.6 for pure H_2O as well as for reasonably dilute solutions, the isotope composition dependence of γ_e for H_2O, HDO, and D_2O can be calculated by varying the $\delta\upsilon_{ht}$ values with χ_D as in section 2.3.1. The calculated γ_e for H_2O, HDO, and D_2O as a function of χ_D are shown in Figure 5, where frequency shifts are allowed either for υ_{ht} only or for both υ_{ht} and υ_{lib}. In both cases, the γ_e were calculated via reference to the respective pure liquid vapor pressures. (For HDO, we assume that $p_{sat}(HDO)\cdot\alpha_{eqm} = p_{sat}(H_2O)$, where α_{eqm} is the H_2O/HDO equilibrium fractionation factor.)

When the $\delta\upsilon_{ht}$ are specified such that $\delta\upsilon_{ht}(H_2O) = -\delta\upsilon_{ht}(D_2O)$ at each χ_D (referenced to the values given in Table 2), the calculated γ_e for H_2O and D_2O both vary by approximately a factor of 2 with composition; both are smallest for the respective pure solutions but are calculated to be somewhat larger than 1 when the isotopomer exists as a trace species. γ_e(HDO) is largest when $\chi_D \sim 0.5$ and decreases toward both high and low deuterium concentrations.

To our knowledge, no measurements of either the pure liquid water surface spectrum or the bulk liquid spectrum as a function of isotopic composition in the librational or hindered translational regions exist to facilitate the determination of how the υ_{ht} (or υ_{lib}) might vary with changing isotopic composition. Furthermore, even if such measurements did exist, the complex and overlapping nature of the spectroscopic features might preclude an explicit determination of any such isotopic variability. We therefore stress that the above analysis is meant only to provide a physical rationale for the observed χ_D dependence of α_{evap} (viz., that small frequency shifts in the hindered translational and librational frequencies with χ_D can have a dramatic affect on the observed free evaporation fractionation) and to establish to what extent these calculations are consistent with measurements of γ_e. Direct measurements of γ_e for pure D_2O are currently underway in our lab and should provide further insights into our understanding of liquid water evaporation.

Despite the inherent difficulties and uncertainties in calculating γ_e, the evaporation model indicates that the absolute magnitude of γ_e is highly sensitive to the nature of the surface environment. Thus, the presence of any impurities (either inorganic or organic) might have a strong influence on the γ_e. This has potentially important consequences for the modeling of cloud formation and the understanding of measurements of cloud condensation nuclei (CCN) in the atmosphere. There has been significant debate over the "best" value to use for the mass accommodation coefficient in cloud models, and quite often a value of ∼0.045 has been used, significantly lower than the values measured by either Smith et al. or Li et al.[2,3,26] The need for use of a lower value in cloud models does not necessarily indicate that the fundamental value for water is in fact lower, but very likely reflects the influence of impurities on water mass transfer in the atmosphere.[27] On the basis of our results, we suggest that use of a variable value for the mass accommodation coefficient of water, which depends in some manner on the local chemical environment, might allow for a more complete description of cloud dynamics in models. Simple variable uptake models have been considered previously (e.g., Lance et al.);[28] however, further research will be necessary to establish the explicit nature of this variability.

3. Equilibrium Fractionation Versus Fractionation During Free Evaporation

Our experimental results indicate that, for the unidirectional process of evaporation from water, the extent of isotopic fractionation depends explicitly on the isotopic composition. This conclusion is supported by the results from the TST model developed above. Furthermore, the model calculations suggest that in general $\gamma_e(H_2O) \neq \gamma_e(D_2O) \neq \gamma_e(HDO)$. At equilibrium, it is required that the microscopic evaporation and condensation fluxes of the individual water isotope species across the surface

are equal and that there is no net transport of water molecules between the vapor and the condensed phase, for example, $J_{e,H_2O} = J_{c,H_2O}$. However, there is no requirement that in an isotopic mixture the evaporation and condensation fluxes of the different isotopic species are equal, for example, $J_{e,H_2O} \neq J_{e,HDO}$, nor that, for example, $\gamma_e(H_2O) = \gamma_e(HDO)$. (Actually, if $\gamma_e(H_2O) = \gamma_e(HDO)$ the isotopic fluxes still need not be equal because $J_{e,max}$ depends on p_{sat}, which is different for the different isotopic species.) Because γ_e is a kinetic parameter, it will not play a role in determining the magnitude of the equilibrium fractionation factors. It is, therefore, the respective partial pressures of the water isotopomers that determine the equilibrium fractionation factor, independent of γ_e. Thus, we might picture liquid−vapor equilibrium of an isotopic mixture (or any mixture) as follows: the microscopic rates of transport across the liquid−vapor interface are determined by the evaporation coefficients and the fundamental nature of the liquid surface, but the equilibrium vapor composition depends only on the bulk thermodynamic parameters. This suggests that, if the composition of the vapor above a liquid mixture were monitored as the equilibrium state were approached, the different mixture components would approach their equilibrium values at different rates dependent on both the saturation vapor pressure and the evaporation coefficient.

In our experiments described in ref 1, the system is far from equilibrium, and therefore, we probe the theoretical, instantaneous approach to equilibrium for the respective isotopic solution. Because there is negligible recondensation in these liquid microjet experiments, the absolute value of γ_e is a controlling factor in determining the evaporation rate. The basic thermodynamically determined differences in p_{sat} between the different isotopic species set baseline values for the expected magnitudes of isotopic fractionation, but it is the explicit differences in γ_e at every χ_D that determine the actual extent of fractionation for this system.

4. Conclusions

We have interpreted our prior measurements[1] of evaporation of liquid water under conditions wherein free molecular evaporation dominates through the development of a model of evaporation based on transition state theory. The strong dependence of α_{evap} on the liquid isotopic composition reflects the sensitivity of evaporating water molecules to the nature of the first hydration shell. This dependence has been explained in terms of small shifts in the relative surface librational and hindered translational frequencies of the water isotopomers with isotopic composition. Comparisons with calculations of the equilibrium fractionation factor suggest that the intermolecular frequencies of the surface molecules may be much more sensitive than the bulk liquid counterparts to changes in isotopic composition.

The model analysis also indicates that the pre-factor for evaporation may be temperature dependent. Recognizing this, the measured[1] T dependence of α_{evap} was reconsidered. Specifically, our previous interpretation of the slope in a plot of ln α_{evap} versus $1/RT$ as the difference in the activation energies between different water isotopomers was probably too simplistic because there is an additional contribution from the pre-factor T dependence. However, the isotope dependent trends in the model calculations of $\alpha_{evap}(T)$ are highly consistent with the observations, although there is a lack of quantitative agreement between the calculated and the observed slopes.

It is not possible to a priori calculate the evaporation rate for liquid water because not all of the necessary terms are known. However, the evaporation model can nonetheless be used to explore the temperature variation of free evaporation, and specifically of the evaporation coefficient. The model provides an explanation for the very small variation in γ_e with temperature for liquid H_2O observed by Smith et al.,[2] given an appropriate choice of the activation energy for evaporation. In this case, the calculated T dependence of the liquid water evaporation rate is actually very similar to ΔH_{vap} and is reasonably consistent with our previous observations. When E_a is specified instead to agree with the strong negative variation of the mass accommodation coefficient with temperature as observed by Li et al.,[3] the calculated T dependence of the evaporation rate is significantly smaller. Further measurements are necessary to resolve the disparity between these studies.

Our results also demonstrate the extreme sensitivity of γ_e to composition, suggesting that the use of a variable γ_e in, for example, cloud models may be desirable as trace impurities could potentially engender dramatic changes in γ_e, although further experimental and theoretical work is necessary to explicitly determine how γ_e depends on solution composition.

Appendix A

Influence of Surface Isotope Gradients. In the above discussion, as previously discussed,[1] we have assumed that the isotopic ratios at the liquid surface are the same as those in the bulk liquid, that is, that there is negligible fractionation in transferring the molecules between the bulk and the liquid surface. However, there has been some concern that there may have been a significant isotope gradient at the liquid surface established during our experiments, which could have influenced the observed α_{evap}. We consider the potential implications of this assumption by qualitatively considering what effect the establishment of a near-surface isotope gradient might have had on our experiments. We assume that the surface isotopic composition was equal to the bulk composition just as the liquid jet left the nozzle. At this point, preferential fractionation of one isotopomer over another might have led to an isotopic gradient. If the evaporation rate for H_2O was greater than that for D_2O and HDO (because $\alpha_{eqm} > 1$), then the surface would have become somewhat enriched in deuterium, eventually approaching steady state with $(D/H)_{surface} > (D/H)_{bulk}$. At every time after the liquid sample was exposed to vacuum, the D/H ratio at the liquid surface would have become larger than that in the bulk. Thus, there would have been proportionally a greater number of D_2O and HDO molecules occupying surface sites than H_2O molecules. Such a process would actually have led to a smaller observed α for all values of χ_D; that is, at no time should an isotope gradient have led to the observation that $\alpha_{evap} > \alpha_{eqm}$. For small χ_D, we did observe that $\alpha_{evap} < \alpha_{eqm}$, which could possibly have been the result of there being an isotopic gradient. However, for large χ_D, we measured $\alpha_{evap} > \alpha_{eqm}$ which, if the establishment an isotopic gradient were the source of this result, would indicate that $(D/H)_{surface} < (D/H)_{bulk}$. Thus, it is clear that any near-surface isotopic gradient that would have been established (assuming that $\alpha_{eqm} = \alpha_{evap}$ or that α_{evap} is constant with χ_D) cannot explain our observations.

Appendix B

Calculating Equilibrium Fractionation Factors. Bigeleisen demonstrated that it is possible to approximately calculate the liquid−vapor equilibrium fractionation factor for water from theory, given knowledge of the internal and external frequencies

of the vapor phase and the liquid:[29]

$$\ln\alpha_{eqm} \sim \ln\frac{p_L}{p_H} = \ln\frac{Q_g^L}{Q_g^H}\frac{Q_c^H}{Q_c^L} + \frac{p_L V_L - p_H V_H}{RT} + G^{**} \quad \text{(A1)}$$

The second two terms on the right-hand side are corrections for molar volume and nonideality and are typically ignored because they are reasonably small. Q_c is the partition function for the bulk condensed phase and Q_g is the partition function for the gas phase. The L and H stand for the light and heavy isotopomers, respectively. Given our above treatment of the transition state as a gas-phase molecule with 2 degrees of freedom and of the surface species, the expression for α_{eqm} is very similar to that for α_{evap}. Thus, under the harmonic oscillator approximation

$$\alpha_{eqm} \approx \frac{Q_g^L}{Q_g^H}\frac{Q_c^H}{Q_c^L} = \left(\frac{M_L}{M_H}\right)^{3/2}\left[\frac{I_A^L I_B^L I_C^L}{I_A^H I_B^H I_C^H}\right]^{1/2}\prod_{i=1}^{3}\left(\frac{1-e^{-u_{i,g}^H}}{1-e^{-u_{i,g}^L}}\right)\prod_{i=1}^{9}\left(\frac{1-e^{-u_{i,c}^H}}{1-e^{-u_{i,c}^L}}\right)e^{-\Delta E_a/kT} \quad \text{(A2)}$$

where $u = h\nu/kT$. The term $\exp(-\Delta E_a/kT)$ is necessary in order to account for the ZPE differences between the respective isotopomers, as it has been previously argued that the bottom of the potential well is the appropriate choice of reference state in this case because it is independent of isotopic identity.[11]

Importantly, we note that eq A2 is not equivalent to the commonly used expression for α_{eqm} under the harmonic oscillator approximation as given by Bigeleisen and reproduced by Van Hook.[12] In particular, in the Bigeleisen formulation, the calculated α_{eqm} is reported to have an additional linear dependence on the ratios of both the gas phase and the condensed phase frequencies. The linear dependence on the gas-phase frequencies arises from application of the Teller−Redlich rule, which relates the isotopic ratios for molecular mass and moments of inertia to the vibrational frequencies, that is

$$\left(\frac{M_H}{M_L}\right)^{3/2}\left[\frac{(I_A^H I_B^H I_C^H)^{1/2}}{(I_A^L I_B^L I_C^L)^{1/2}}\right] = \prod_i^N\left(\frac{m_i^H}{m_i^L}\right)^{3/2}\prod_i^{3N-6}\left(\frac{\nu_i^H}{\nu_i^L}\right) \quad \text{(A3)}$$

The origin of the linear dependence on the condensed phase frequencies is not clearly stated in the original derivation presented in ref 29. Direct application of the vibrational, translational, and rotational partition function relationships expressed in section 2.1 to determination of α_{eqm} from eq A1 does not substantially slow the calculation on modern computers making these approximations unnecessary.

The α_{eqm} calculated from eq A2 exhibit similar sensitivities to errors, shifts, or both in the condensed phase intermolecular isotope frequency differences as α_{evap}, as expected on the basis of their similar formulations. In contrast, use of the Bigeleisen expression for α_{eqm} indicates there is a negligible dependence on the intermolecular isotope frequency differences and an unreasonably strong dependence on the specification of the intramolecular isotope frequency differences. This is a consequence of the Bigeleisen expression having a linear dependence on the condensed phase frequencies which dampens the influence of the low-frequency modes and makes the internal contributions to fractionation unrealistically large.

Using the bulk liquid frequencies specified above in the TST model of evaporation (and assuming ν_{ht} is isotope independent), we calculate that $\alpha_{eqm} = 0.95$ (H_2O/HDO) and $\alpha_{eqm} = 1.01$ (H_2O/D_2O) at 295 K. These calculated values differ from the experimental values of $\alpha_{eqm} = 1.083$ (H_2O/HDO) and $\alpha_{eqm} = 1.165$ (H_2O/D_2O).[30] However, exact agreement between calculation and experiment can be found by varying the estimated bulk frequencies by very small amounts (e.g., $\delta\nu_{ht}(H_2O) = -\delta\nu_{ht}(D_2O) = 2.7\ cm^{-1}$, $\delta\nu_{ht}(HDO) = -2.1\ cm^{-1}$). Importantly, the calculations reproduce well the known temperature dependencies of the α_{eqm} (i.e., the slope of a plot of $\ln\alpha_{eqm}$ vs $1/RT$), yielding 0.8 kJ/mol and 1.6 kJ/mol for H_2O/HDO and H_2O/D_2O fractionation, respectively, in perfect agreement with experimental values.

Variables and Terms

α_{evap}	evaporation fractionation factor
α_{eqm}	equilibrium fractionation factor
δ_v	frequency shift (cm^{-1})
χ_D	deuterium mole fraction
γ_e	evaporation coefficient
θ_x	rotational temperature (K)
s	symmetry factor for rotation
area	area of 2D transition state (m^2)
A_x	pre-factor
I_x	moment of inertia ($kg\cdot m^2$)
E_a	activation energy (kJ/mol)
ΔE_a	activation energy difference (kJ/mol)
J_e	evaporation rate ($molecules\cdot m^{-2}\cdot s^{-1}$)
R_x	isotopic ratio
Q^*	total partition function for the transition state
Q_s	total partition function for the surface species
H	heavy isotopomer
L	light isotopomer
q_v	vibrational partition function
q_r	rotational partition function
q_t	vibrational partition function
q_{lib}	librational partition function
q_{ht}	hindered translational partition function
ν_i	vibrational frequency (cm^{-1})
k	Boltzmann's constant ($J\cdot K^{-1}$)
T	temperature (K)
m	molecular mass (kg)
R	ideal gas constant ($J\cdot mol^{-1}\cdot K^{-1}$)
h	Plank's constant ($J\cdot s$)

Acknowledgment. This research was supported by the National Science Foundation Atmospheric Chemistry Program under Grant ATM-0138669 (RCC) and the Chemical Sciences, Geosciences and Biosciences Division, Office of Basic Energy Sciences, U.S. Department of Energy (R.J.S.). C.D.C. was supported by the Advanced Light Source Doctoral Fellowship in Residence and the National Defense Science and Engineering Graduate Fellowship. We thank the anonymous reviewers for comments that greatly improved the paper.

References and Notes

(1) Cappa, C. D.; Drisdell, W.; Smith, J. D.; Saykally, R. J.; Cohen, R. C. *J. Phys. Chem. B* **2005**, *109*, 24391.

(2) Smith, J. D.; Cappa, C. D.; Drisdell, W. S.; Cohen, R. C.; Saykally, R. J. *J. Am. Chem. Soc.* **2006**, *128*, 12892.

(3) Li, Y. Q.; Davidovits, P.; Shi, Q.; Jayne, J. T.; Kolb, C. E.; Worsnop, D. R. *J. Phys. Chem. A* **2001**, *105*, 10627.
(4) Shaw, R. A.; Lamb, D. *J. Chem. Phys.* **1999**, *111*, 10659.
(5) Winkler, P. M.; Vrtala, A.; Wagner, P. E.; Kulmala, M.; Lehtinen, K. E. J.; Vesala, T. *Phys. Rev. Lett.* **2004**, *93*, 075701.
(6) Smith, J. A.; Livingston, F. E.; George, S. M. *J. Phys. Chem. B* **2003**, *107*, 3871.
(7) Redondo, A.; Zeiri, Y.; Low, J. J.; Goddard, W. A. *J. Chem. Phys.* **1983**, *79*, 6410.
(8) Benedict, W. S.; Gailar, N.; Plyler, E. K. *J. Chem. Phys.* **1956**, *24*, 1139.
(9) Eisenberg, D. S.; Kauzmann, W. *The structure and properties of water;* Clarendon P.: Oxford, 1969.
(10) Atkins, P. W. *Physical Chemistry;* W. H. Freeman and Company: New York, 1998.
(11) Bigeleisen, J.; Mayer, M. G. *J. Chem. Phys.* **1947**, *15*, 261.
(12) Van Hook, W. A. *J. Phys. Chem.* **1968**, *72*, 1234.
(13) Wolfsberg, M.; Massa, A. A.; Pyper, J. W. *J. Chem. Phys.* **1970**, *53*, 3138.
(14) Smith, J. D.; Cappa, C. D.; Wilson, K. R.; Cohen, R. C.; Geissler, P. L.; Saykally, R. J. *Proc. Natl. Acad. Sci. U.S.A.* **2005**, *102*, 14171.
(15) These frequencies were determined from measurements performed in this laboratory.
(16) Maréchal, Y. *J. Chem. Phys.* **1991**, *95*, 5565.
(17) Du, Q.; Superfine, R.; Freysz, E.; Shen, Y. R. *Phys. Rev. Lett.* **1993**, *70*, 2313.
(18) Moskovits, M.; Michaelian, K. H. *J. Chem. Phys.* **1978**, *69*, 2306.
(19) Walrafen, G. E.; Blatz, L. A. *J. Chem. Phys.* **1973**, *59*, 2646.
(20) Van Hook, W. A. *J. Phys. Chem.* **1972**, *76*, 3040.
(21) McGuire, J. A.; Shen, Y. R. *Science,* **2006**, *313*, 1945.
(22) Speedy, R. J.; Debenedetti, P. G.; Smith, R. S.; Huang, C.; Kay, B. D. *J. Chem. Phys.* **1996**, *105*, 240.
(23) Carey, D. M.; Korenowski, G. M. *J. Chem. Phys.* **1998**, *108*, 2669.
(24) Fukuta, N.; Walter, L. A. *J. Atmos. Sci.* **1970**, *27*, 1160.
(25) Seinfeld, J. H.; Pandis, S. N. *Atmospheric chemistry and physics: from air pollution to climate change;* Wiley: New York, 1998.
(26) Pruppacher, H. R.; Klett, J. D. *Microphysics of clouds and precipitation*, 2nd ed.; Kluwer Academic Publishers: Boston, MA, 1996.
(27) McFiggans, G.; Artaxo, P.; Baltensperger, U.; Coe, H.; Facchini, M. C.; Feingold, G.; Fuzzi, S.; Gysel, M.; Laaksonen, A.; Lohmann, U.; Mentel, T. F.; Murphy, D. M.; O'Dowd, C. D.; Snider, J. R.; Weingartner, E. *Atmos. Chem. Phys.* **2006**, *6*, 2593.
(28) Lance, S.; Nenes, A.; Rissman, T. A. *J. Geophys. Res.* **2004**, *109*.
(29) Bigeleisen, J. *J. Chem. Phys.* **1961**, *34*, 1485.
(30) Jancso, G.; Vanhook, W. A. *Chem. Rev.* **1974**, *74*, 689.